Preparation of PVDF/PEI double-layer composite hollow fiber membranes for enhancing tensile strength of PVDF membranes

Jun-Gui Yuan, Bao-Li Shi [*] and Ling-Yun Ji

Department of Chemistry, College of Science, Northeast Forestry University, Harbin 150040, PR China

Abstract. Polyvinylidene fluoride (PVDF) hollow fiber membrane is widely used for water treatment. However, the weak mechanical strength of PVDF limits its application. To enhance its tensile strength, a double-layer composite hollow fiber membrane, with PVDF and polyetherimide as the external and inner layers, respectively, was successfully prepared through phase inversion technique. The effects of additive content, air gap distance, N,N-dimethyl-acetamide content in the inner core liquid, and the temperature of external coagulation bath on the membrane structure, permeation flux, rejection, tensile strength, and porosity were determined. Experimental results showed that the optimum preparation conditions for the double-layer composite hollow fiber membrane were as follows: PEG-400 and PEG-600, 5 wt%; air gap distance, 10 cm; inner core liquid and the external coagulation bath should be water; and temperature of the external coagulation bath, 40 C. A single layer PVDF hollow fiber membrane (without PEI layer) was also prepared under optimum conditions. The double-layer composite membrane remarkably improved the tensile strength compared with the single-layer PVDF hollow fiber membrane. The permeation flux, rejection, and porosity were also slightly enhanced. High-tensile strength hollow fiber PVDF ultrafiltration membrane can be fabricated using the proposed technique.

Keywords: PVDF; PEI; ultrafiltration; tensile strength

1. Introduction

Ultrafiltration (UF) was discovered in the 19th century and became well-developed in the 20th century. UF is an efficient wastewater treatment technique applied in various industries, including energy, environmental, chemical, electronic, and biotechnological areas, because of its suitable pore size (usually ranging from 2 nm to 50 nm), and it can remove organic contaminant and emulsified oil (Tian *et al.* 2013, Hamza *et al.* 1997). UF membranes are also widely applied in membrane bioreactors (MBRs) because of its high volumetric loading rate capability, small floor space, effluent quality, and good disinfection. UF membranes may be classified into hollow fiber, flat sheet, and multi tubular membranes (Castaing *et al.* 2010, Arevalo *et al.* 2012).

Polyvinylidene fluoride (PVDF) is a family of hydrophobic thermoplastic with alternating -CH_2 and -CF_2 groups along the polymer chains. PVDF membranes has been regarded as one of the

---

most interesting membrane materials in the ultrafiltration industry because of their outstanding chemical resistance, well-controlled porosity, high organic selectivity, membrane forming property, and good thermal property (Sun *et al.* 2013, Zhang *et al.* 2009, Sukitpaneenit and Chung 2009). Hollow fiber membranes have some advantages, such as high surface to volume ratio, less demand for pretreatment and maintenance, and no separation requirement between the feed and permeate solution. Hollow fiber membranes are widely applied in various areas, such as in bio-separation, drinking water purification, wastewater treatment, and gas separation (Yu *et al.* 2012, Kola *et al.* 2012, Feng *et al.* 2013). Until now, PVDF hollow fiber ultrafiltration membrane has been widely used in waste water treatment field such as MBR technique, because of its good anti-fouling property. However, the weak tensile strength of PVDF UF hollow fiber membranes limits the working capacity and application ranges of these membranes. Hence, the improvement of the tensile strength of PVDF hollow fiber membranes is particularly urgent.

Numerous methods including physical blending (Pezeshk and Narbaitz 2012, Li *et al.* 2010, Wei *et al.* 2011), chemical grafting (Liu *et al.* 2011), and surface modifying (Li *et al.* 2013) have been investigated to improve membrane performance. One of the most popular techniques for hollow fiber membrane preparation is the immersion precipitation (IP) method, in which the polymer solution is immersed in a coagulation bath that contains a non-solvent. The solvent–non-solvent exchange occurs during the liquid–liquid demixing process. This exchange induces the casting solution phase separation to form polymer-rich and polymer-lean phases; thereby, the membrane is formed (Ahmad *et al.* 2011, Zhang *et al.* 2010a, Mansourizadeh and Ismail 2011). The chosen polymer, solvent, non-solvent system, and their compositions affect the morphology and performance of the membrane. In addition, the non-solvent additives, coagulant bath temperature and composition, casting speed, atmosphere, and air gap distance can influence the formation of the membrane.

A double-layer composite hollow fiber membrane is a special membrane with a thin dense skin layer and porous support layer prepared by different polymers. In general, the porous support layer was prepared first through the IP method. Subsequently, the dense shin layer was prepared through the dip coating process, interfacial polymerization, and plasma polymerization. The dense skin layer has a chief function in the UF process (Balachandra *et al.* 2003). Therefore, the tensile strength of PVDF hollow fiber membrane may be enhanced by preparing a double-layer composite membrane, if another polymer with higher tensile strength is chosen.

Polyetherimide (PEI) is one of the most popular polymers for asymmetric membrane preparation because of its excellent membrane forming ability, solvent resistance, high selectivity, good thermal resistance, and good mechanical properties (Chinpa *et al.* 2010, Zhang *et al.* 2011). PEI membranes are widely used in gas separation, liquid mixture evaporation separation, and biomedical applications (Zhang *et al.* 2010b). We found that PEI and PVDF could dissolve in DMAC, forming a homogeneous solution without layering. It means that PEI and PVDF have a good compatibility and they can be used to prepare double-layer composite membrane at some conditions. The aim of the present study was to fabricate a double-layer composite membrane with PVDF and PEG-400 as the external membrane spinning solution, and with PEI and PEG-600 as the internal membrane spinning solution to enhance the tensile strength of the PVDF hollow fiber membranes. The internal and external membrane layers were fabricated simultaneously through double-layer spinneret by phase inversion technique. The effects of the additive content, air gap distance, N,N-dimethyl-acetamide (DMAC) content in the inner core liquid, and the external coagulation bath temperature on membrane structure, permeation flux, rejection, tensile strength, and porosity were determined.

2. Experiment

2.1 Materials

PVDF6010 and PEI1000-1000 were used as membrane materials. PVDF was purchased from Solvay, Belgium. PEI was purchased from Saudi Basic Industry Corporation, Saudi Arabia. DMAC (AR) was used as solvent and purchased from Tianjin Kermel Chemical Reagents Development Center, China. The non-solvent additives used in the polymer dopes were PEG-400 and PEG-600, which were purchased from Tianjin Guangfu Fine Chemical Research Institute, China. Bovine serum albumin (BSA, molecular weight: 68,000 $g \cdot mol^{-1}$) was purchased from Beijing AoBoXing Bio-tech Co., Ltd., China. Distilled water was used as coagulation bath medium for the spinning process.

2.2 Preparation of hollow fiber membrane

The hollow fiber membranes were prepared through dry-jet wet spinning process. The polymer was dried at 60°C under vacuum for at least 24 h before usage. One spinning dope contained 18 wt% PVDF and 5 wt% PEG-400. Another dope contained 13 wt% PEI and 5 wt% PEG-600. The mixtures were stirred at 60°C using a magnetic stirrer for approximately 4 h to 5 h to form homogeneous spinning dopes. Afterward, the dopes were degassed at 60°C. The PVDF spinning dope was used as the outer dope solution, and PEI spinning dope was used as the inner dope solution. The spinning dopes were forced out by N_2 at a controlled rate and went through a certain air gap distance before immersion in the coagulation bath. Distilled water was used as both the inner core liquid and the external coagulation bath. The prepared hollow fiber membranes were stored in a distilled water bath to remove residual solvent for at least 24 h before further measurements. The schematic presentation of spinning for the preparation of the double-layer composite hollow fiber membrane is shown in Fig. 1, and the spinning parameters are listed in Table 1.
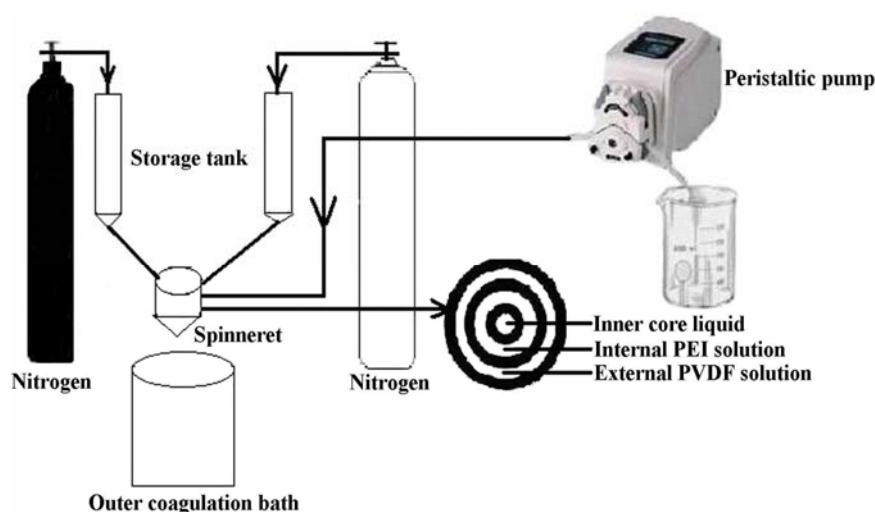

Fig. 1 Spinning schematic of double-layer hollow fiber membrane

Table 1 Spinning parameters for hollow fiber membrane

Spinneret o.d/i.d.(mm)	1.10/0.55
Inner core liquid	Distilled water or mixture of water/DMAC
Flow rate of inner core liquid (mcL/min)	4
Air gap distance (cm)	1/5/ 10 /15
External coagulation bath	Distilled water
External coagulation bath temperature (ºC)	20/30/40/50
Spinning dope temperature (ºC)	20

2.3 Tensile strength measurement

The tensile strength of the hollow fiber membranes was measured by using an electronic fiber strength machine (YG162D/E, Wenzhou Jigao Testing Instrument Co. Ltd., China) at room temperature. The inner and external diameters of the membranes were detected using an electronic magnifier to calculate the cross-sectional area. All samples were cut to 10-cm long portions at wet state. Ten samples were measured, and the average tensile strength was obtained. The relative standard deviation of tensile strength was less than 10%.

2.4 Membrane porosity measurement

Membrane porosity was measured by weighing the dry and wet mass of the membranes. Ten 10-cm long hollow fibers were immersed into distilled water for at least 24 h at room temperature. The wet membranes were weighed after removing the remaining water from the inner surface using air flow and after wiping the water from the outer surface of the membrane using a filter paper. Then, the wet membranes were dried in a vacuum at 60°C for 24 h and weighed. Membrane porosity was calculated using the following equation

$$\varepsilon = \frac{w_1 - w_2}{\rho_w \times A \times l} \tag{1}$$

where ε is the membrane porosity (%), w_1 is the wet membrane weight (g), w_2 is the dry membrane weight (g), ρ_w is the water density (g/cm^3), A is the membrane effective area (cm^2), which was calculated with the inner or external diameter and the length of hollow fiber membrane, and l is the membrane thickness (cm). Five samples were measured for each kind of hollow fiber membrane. The relative standard deviation was less than 10%, and the average porosity value was obtained.

2.5 Permeation flux and rejection of membranes

The permeation flux and rejection of membranes were measured using a self-made, dead-end filtration equipment at room temperature and 0.1 MPa. Before permeation collection, the membrane was compressed under 0.15 MPa for 20 min to obtain a steady flux. Permeation flux was measured after the steady state was reached. The rejection test was performed using 0.1 g·L^{-1} BSA solution. The absorbance of the feed and permeation of BSA solution was measured using a UV-VIS spectrophotometer (T6, Beijing Purkinje General Instrument, China) at 280 nm

wavelength. The BSA concentration was calculated from the absorbance working curve. At least three measurements were performed to obtain an average value. The permeation flux was calculated using the following equation

$$F = \frac{V}{At} \tag{2}$$

where F is the permeation flux ($L \cdot m^{-2} \cdot h^{-1}$), V is the permeation volume (L), A is the inner surface area of the hollow fiber membrane (m^2) which was calculated with the inner diameter and the length of hollow fiber membrane, and t is the permeation time (h). Rejection rate is defined through the following equation

$$R = \left(1 - \frac{C_P}{C_f}\right) \times 100\% \tag{3}$$

where R is the rejection rate (%), C_p is the permeate concentration, and C_f is the feed BSA solution concentration. The relative standard deviation of flux and rejection was both less than 10%.

2.6 Morphology characterization of membranes

The cross-section morphology of the hollow fiber membranes was observed using a scanning electron microscope (SEM, FEI Sirion, Holland) through the standard method. The membrane samples were immersed in liquid nitrogen and fractured carefully. The samples were then dried in vacuum and coated before the test, using a thin layer of sputtered gold.

2.7 Viscosity measurement

The viscosity of the spinning dope was measured using a digital viscometer (NDJ-5S, Shanghai Jingtian Electronic Instrument Co. Ltd., China). The completely dissolved homogeneous spinning dopes were stirred with the spindle of the digital viscometer at the rotation speed of 30 r/min at room temperature. At least ten times were measured for each kind of spinning dope, and the average viscosity value was obtained.

3. Results and discussion

3.1 Effect of additive content on membrane performance

Table 2 lists the tensile strength of the single layer and double-layer hollow fiber membranes. It is obvious that the tensile strength of the single layer PEI hollow fiber membrane is stronger than the single layer PVDF hollow fiber membrane. All of the tensile strength of the double-layer composite membranes is improved compared with the single layer PVDF membrane.

The effect of the additive content on the tensile strength is also demonstrated in Fig. 2. The red and green points represent the experimental data. The gray surface is calculated from the experimental data with Design-Expert 8.0 (a response surface methodology software), which reflects an approximate relationship between the influence factor and the experimental data (Zou *et al.* 2012). The red and green points are above and below the surface, respectively. The tensile strength initially decreases and then increases with increasing PEG-400 and PEG-600 content. The tensile strength changes slightly when PEG-400 and PEG-600 content increases from 5 wt% to

Table 2 Tensile strength of the membrane

Type of membrane	Tensile strength(MPa)
18%PVDF + 5%PEG400	1.03 ± 0.12
13%PEI + 5%PEG600	5.64 ± 0.15
A + 1%PEG400	1.68 ± 0.10
A + 3%PEG400	1.34 ± 0.13
A + 5%PEG400	1.91 ± 0.15
A + 7%PEG400	1.92 ± 0.11
A + 9%PEG400	1.96 ± 0.11
1%PEG600 + B	1.54 ± 0.13
3%PEG600 + B	1.51 ± 0.09
5%PEG600 + B	1.91 ± 0.15
7%PEG600 + B	1.92 ± 0.14
9%PEG600 + B	1.94 ± 0.12

A: 13%PEI + 5%PEG600 + 18%PVDF; B: 13%PEI + 18%PVDF + 5%PEG400

Fig. 2 Effect of additive content on tensile strength

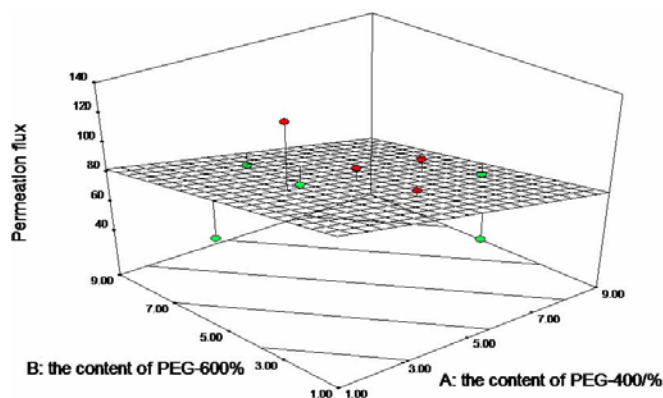Fig. 3 Effect of additive content on porosity

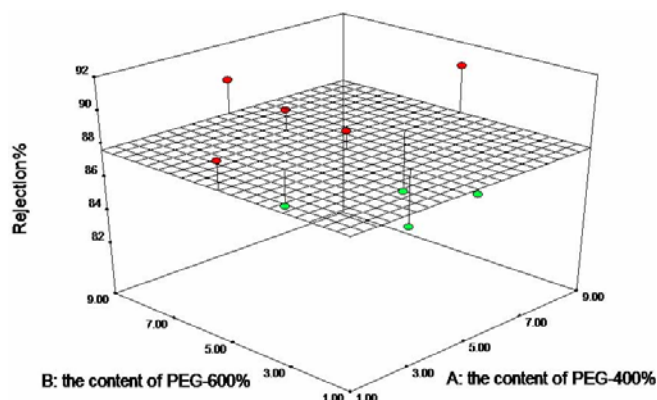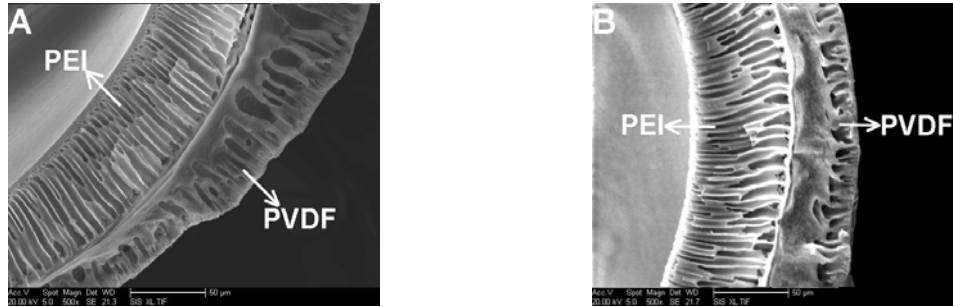Fig. 4 Effect of additive content on permeation flux

Fig. 5 Effect of additive content on permeation flux

9 wt%. Fig. 3 shows the effect of the additive content on porosity. The porosity first increases and then decreases with increasing PEG-400 and PEG-600 content.

The effect of the additive content on the permeation flux is demonstrated in Fig. 4. This diagram shows that the permeation flux first increases and then decreases with increasing PEG-400 and PEG-600 content. On the contrary, the rejection rate initially decreases and then increases with increasing PEG-400 and PEG-600 content (Fig. 5). The optimum additive content is 5 wt% for the PEG-400 and PEG-600 additives.

The influence of the additive content on the cross-section morphology of the membrane is illustrated in Fig. 6. The inner PEI membrane has finger-like structure, and a dense skin layer is found in the inner surface of the PEI membrane. However, the PVDF membrane consists of large pores and sponge-like structure. The PVDF membrane prepared with 1 wt% PEG-400 has more large pores than the PVDF membrane prepared with 7 wt% PEG-400. However, the PVDF membrane prepared with 7 wt% PEG-400 has a denser sponge-like structure than the PVDF membrane prepared with 1 wt% PEG-400. Table 3 shows the viscosity of spinning dope with different additive content. The viscosity of the spinning dope increases with increasing amount of

(a) PVDF/1 wt%PEG-400 + PEG/5 wt%PEG-600   (b) PVDF/7 wt%PEG-400 + PEG/5 wt%PEG-600

Fig. 6 Cross-section morphology of membranes with different additive contents

Table 3 Viscosity of spinning dope

Spinning dope	Viscosity (MPa·s)
PVDF + 1%PEG400	1416.63 ± 1.31
PVDF + 3%PEG400	1537.09 ± 0.98
PVDF + 5%PEG400	1772.52 ± 1.14
PVDF + 7%PEG400	1829.19 ± 0.60
PVDF + 9%PEG400	1845.86 ± 0.45
PEI + 1%PEG600	256.60 ± 0.12
PEI + 3%PEG600	288.89 ± 0.19
PEI + 5%PEG600	293.44 ± 0.21
PEI + 7%PEG600	315.95 ± 0.29
PEI + 9%PEG600	356.47 ± 0.26

additive. The low viscosity of the spinning dope facilitates the diffusion of the additive into the coagulation bath, which results in the formation of large pores in the cross-section, thereby enhancing the permeation flux. However, the tensile strength decreases when larger pores exist in the membrane.

3.2 Effect of air gap distance on membrane performance

The effect of air gap distance on the performances of the PVDF membranes, which were prepared using 5 wt% PEG-400 and 5 wt% PEG-600 as additives, is illustrated in Figs. 7-8. When air gap distance increases from 1 cm to 5 cm, the porosity apparently increases from 82.25% to 84.33%. However, when air gap distance increases from 5 cm to 15 cm, almost no change was observed on the porosity. The tensile strength changes between 1.32 MPa and 1.91 MPa. The maximum tensile strength of the membrane was obtained when the air gap distance was 10 cm.

The effects of air gap distance on permeation flux and rejection are shown in Fig. 8. As the air gap distance increases, an upward trend in permeation flux and a downward trend in rejection are presented. For the membrane with maximum tensile strength prepared at the 10 cm air gap
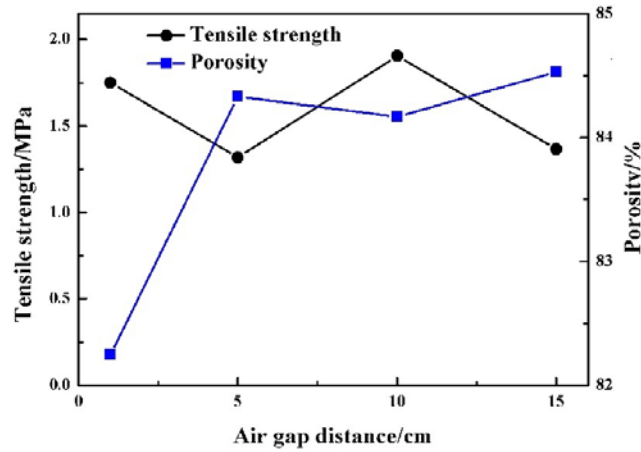
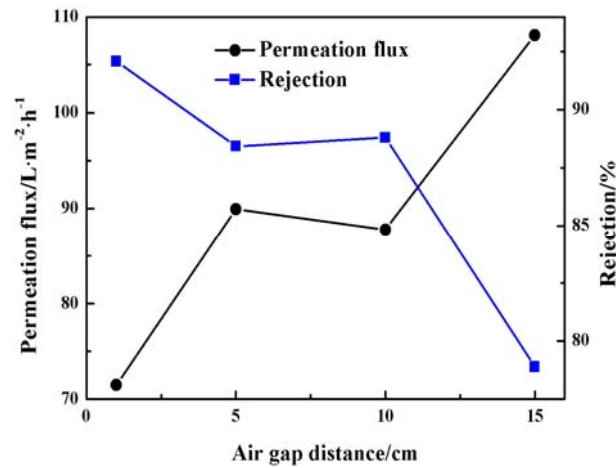Fig. 7 Effect of air gap distance on tensile strength and porosity

Fig. 8 Effect of air gap distance on permeation flux and rejection

distance, the permeation flux and rejection rate have relatively high values of 87.78 $L \cdot m^{-2} \cdot h^{-1}$ and 88.8%, respectively. Therefore, the comprehensive performance of the membrane is better than that of others. Table 4 presents thicknesses of the membranes. When the air gap distance is less than 10 cm, the thickness of the membranes is almost constant. When the air gap distance reaches 15 cm, the thickness of the membrane slightly decreases.

3.3 Effect of DMAC content in inner core liquid on membrane performance

The effects of DMAC content in the inner core liquid on the performance of the PVDF membranes, which were prepared using 5 wt% PEG-400 and 5 wt% PEG-600 as additives and with 10 cm air gap distance, are shown in Figs. 9-10. When DMAC content increases from 0 wt% to 15 wt%, the tensile strength exhibits an upward trend and changes from 1.91 MPa to 2.41 MPa

Jun-Gui Yuan, Bao-Li Shi and Ling-Yun Ji

Table 4 Thickness of membrane with different air gap distance

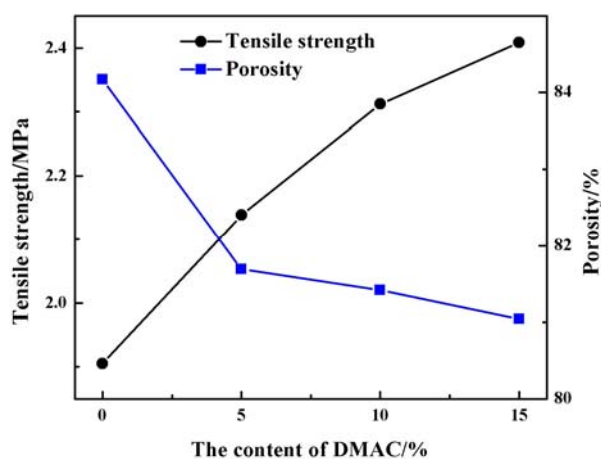| Air gap distance (cm)	Thickness of membrane (mm)
1	0.13 ± 0.01
5	0.13 ± 0.01
10	0.13 ± 0.01
15	0.12 ± 0.01

Fig. 9 Effect of DMAC content in inner core liquid on tensile strength and porosity
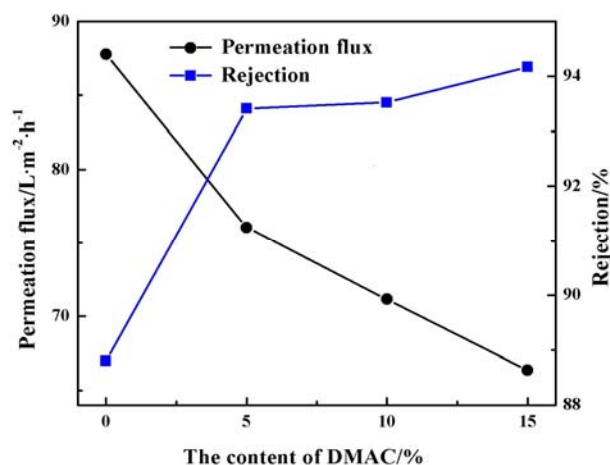

Fig. 10 Effect of DMAC content in inner core liquid on permeation flux and rejection

(Fig. 9). The higher the DMAC content in the inner core liquid, the smaller porosity is formed in the membrane. The effect of DMAC content in the inner core liquid on the permeation flux and rejection is shown in Fig. 10. The permeation flux decreases with increasing DMAC content in the inner core liquid. By contrast, the rejection presents an opposite trend, which increases from

(a) 5 wt%DMAC in inner core liquid   (b) 15 wt%DMAC in inner core liquid
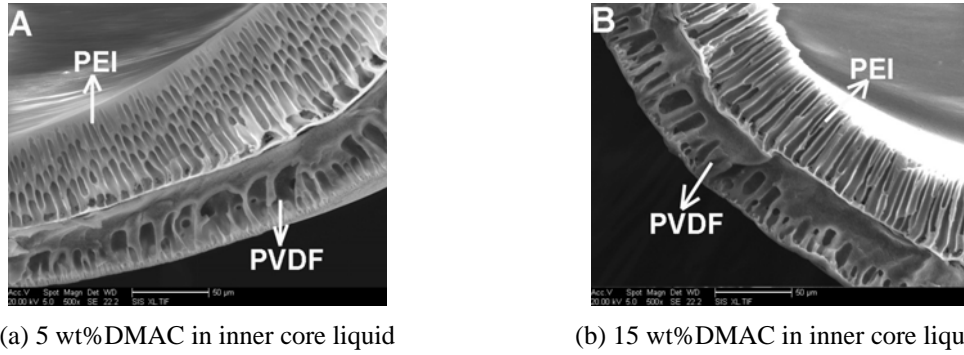
Fig. 11 Cross-section morphology of membranes with different DMAC content in inner core liquid

88.80% to 94.17%. Increasing DMAC content in the inner core liquid leads to the decrease in the precipitation rate when the polymer dope solution comes into contact with the inner core liquid. Therefore, more sponge-like pores appears in the resulting membrane structure, which can be seen in Fig. 11.

3.4 Effect of external coagulation bath temperature on membrane performance

The effects of the external coagulation bath temperature on the performance of the PVDF membranes, which were prepared with 5 wt% PEG-400 and 5 wt% PEG-600 as additives, with 10 cm air gap distance and distilled water as inner core liquid are shown in Figs. 12-13. Porosity increases with increasing external coagulation bath temperature. However, the tensile strength decreases slightly when the temperature changes between 20°C and 40°C. When the temperature reaches 50°C, the tensile strength decreases sharply and reaches a minimum value of 1.80 MPa. The influence of the external coagulation bath temperature on permeation flux and rejection is
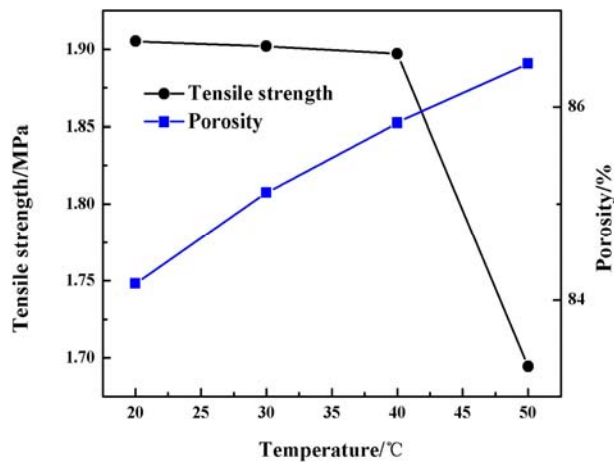

Fig. 12 Effect of external coagulation bath temperature on tensile strength and porosity
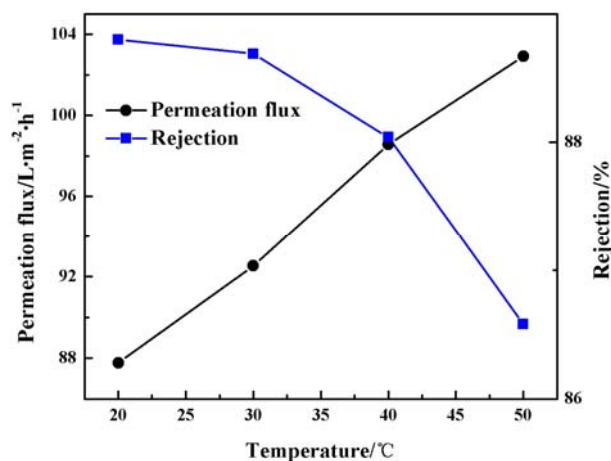
Fig. 13 Effect of external coagulation bath temperature on permeation flux and rejection

shown in Fig. 13. As the external coagulation bath temperature increases, the permeation flux increases, and rejection decreases.

The effect of the external coagulation bath temperature on the cross-section morphology of the membranes prepared at 20°C and 40°C, respectively is shown in Fig. 14. The PVDF membrane prepared at 20°C apparently has more sponge-like structure than the PVDF membrane prepared at 40°C. The time of the delayed phase inversion, which appeared between the dope solution and the external coagulation bath, was longer at 20°C than at 40°C, which resulted in larger areas with the sponge-like structure, but smaller areas with the large pores. Thus, the best external coagulation bath temperature was 40°C.

From the experimental results, we obtained the optimum conditions for the preparation of the double-layer composite PVDF membrane as follows: PEG-400 and PEG-600 additives, 5 wt%; inner core liquid and the external coagulation bath, water; temperature of the external coagulation, 40°C; and air gap distance, 10 cm.
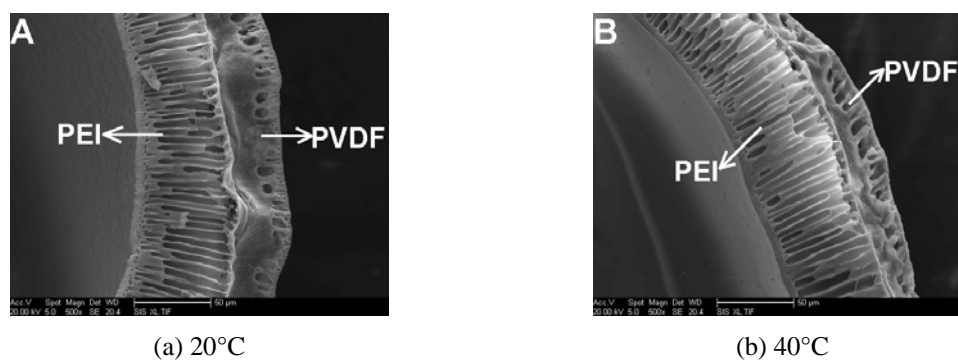

(a) 20°C   (b) 40°C

Fig. 14 Cross-section morphology of membranes prepared at different external coagulation bath temperature

Table 5 Performance of membrane

Type of membrane	PVDF/PEG400	PVDF/PEG400 + PEI/PEG600
Tensile strength (MPa)	1.15 ± 0.05	1.90 ± 0.11
Permeation flux ($L \cdot m^{-2} \cdot h^{-1}$)	59.90 ± 0.33	98.56 ± 0.56
Rejection (%)	86.69 ± 0.01	88.04 ± 0.05
Porosity (%)	77.47 ± 0.51	85.87 ± 0.45

A single-layer PVDF hollow fiber membrane (without PEI layer) was also prepared at the optimum conditions. The membrane properties were measured similar to the double-layer composite PVDF. The performances of these membranes are listed in Table 5. Apparently, all composite membrane performances are higher than that of the single layer PVDF hollow fiber membrane, especially in terms of tensile strength.

4. Conclusions

A double-layer composite hollow fiber membrane was successfully prepared using PVDF and PEI as the external and internal layers, respectively, through one-step phase inversion method. PEG-400 and PEG-600 were used as additives for the PVDF and PEI layers, respectively.

- Experimental results showed that the optimum preparation conditions of the double-layer composite hollow fiber membrane were as follows: PEG-400 and PEG-600 contents, 5 wt%; air gap distance, 10 cm; inner core liquid and the external coagulation, water; and temperature of the external coagulation bath, 40°C.
- A single layer PVDF hollow fiber membrane (without PEI layer) was also prepared under the optimum conditions. The double-layer composite membrane was found to remarkably improve the tensile strength, compared with the single layer PVDF hollow fiber membrane. The permeation flux, rejection, and porosity were also slightly enhanced. High-tensile strength hollow fiber PVDF ultrafiltration membrane can be fabricated using the proposed technique.

Acknowledgments

References

Ahmad, A.L., Ideris, N., Ooi, B.S., Low, S.C. and Ismail, A. (2011), "Morphology and polymorph study of a polyvinylidene fluoride (PVDF) membrane for protein binding: Effect of the dissolving temperature", *Desalination*, **278**(1-3), 318-324.
Arevalo, J., Ruiz, L.M., Albarracin, J.A.P., Perez, D.M.G., Perez, J., Mreno, B. and Gomez, M.A. (2012), "Wastewater resuse after treatment by MBR. Microfiltration or ultrafiltration", *Desalination*, **299**, 22-27.

Balachandra, A.M., Baker, G.L. and Bruening, M.L. (2003), "Preparation of composite membranes by atom transfer radical polymerization initiated from a porous support", *J. Membr. Sci.*, **227**(1-2), 1-14.

Castaing, J.B., Masse, A., Pontie, M., Sechet, V., Haure, J. and Jaouen, P. (2010), "Investigating submerged ultrafiltration (UF) and microfiltration (MF) membranes for seawater pre-treatment dedicated to total removal of undesirable micro-algae", *Desalination*, **253**(1-3), 71-77.

Chinpa, W., Quemener, D., Beche, E., Jiraratananon, R. and Deratani, A. (2010), "Preparation of poly (etherimide) based ultrafiltration membrane with low fouling property by surface modification with poly (ethylene glycol)", *J. Membr. Sci.*, **365**(1-2), 89-97.

Feng, C.Y., Khulbe, K.C., Matsuura, T. and Ismail, A.F. (2013), "Recent progresses in polymeric hollow fiber membrane preparation, characterization and application", *Sep. Purif. Technol.*, **111**, 43-71.

Hamza, A., Pham, V.A., Matsuura, T. and Santerre, J.P. (1997), "Development of membranes with low surface energy to reduce the fouling in ultrafiltration applications", *J. Membr. Sci.*, **131**(1-2), 217-227.

Kola, A., Ye, Y., Ho, A., Clech, P.L. and Chen, V. (2012), "Application of low frequency transverse vibration on fouling limitation in submerged hollow fiber membranes", *J. Membr. Sci.*, **409-410**, 54-65.

Li, N., Xiao, C., An, S. and Hu, X. (2010), "Preparation and properties of PVDF/PVA hollow fiber membranes", *Desalination*, **250**(2), 530-537.

Li, Q., Bi, Q.Y., Lin, H.H., Bian, L.X. and Wang, X.L. (2013), "A novel ultrafiltration (UF) membrane with controllable selectivity for protein separation", *J. Membr. Sci.*, **427**, 155-167.

Liu, F., Abed, M.R.M. and Li, K. (2011), "Preparation and characterization of poly (vinylidene fluoride) (PVDF) based ultrafiltration membranes using nano γ-Al_2O_3", *J. Membr. Sci.*, **366**(1-2), 97-103.

Mansourizadeh, A. and Ismail, A.F. (2011), "Preparation and characterization of porous PVDF hollow fiber membranes for CO_2 absorption: Effect of different non-solvent additives in the polymer dope", *Int. J. Greenh. Gas. Con.*, **5**(4), 640-648.

Pezeshk, N. and Narbaitz, R.M. (2012), "More fouling resistance modified PVDF ultrafiltration membranes for water treatment", *Desalination*, **287**, 247-254.

Sukitpaneenit, P. and Chung, T.S. (2009), "Molecular elucidation of morphology and mechanical properties of PVDF hollow fiber membranes from aspects of phase inversion, crystallization and rheology", *J. Membr. Sci.*, **340**(1-2), 192-205.

Sun, A.C., Kosar, W., Zhang, Y.F. and Feng, X.S. (2013), "A study of thermodynamics and kinetics pertinent to formation of PVDF membranes by phase inversion", *Desalination*, **309**, 156-164.

Tian, J.Y., Ernst, M., Cui, F. and Jekel, M. (2013), "Effect of different cations on UF membrane fouling by NOM fractions", *Chem. Eng. J.*, **223**, 547-555.

Wei, Y., Chu, H.Q., Dong, B.Z., Li, X., Xia, S.J. and Qiang, Z.M. (2011), "Effect of TiO_2 nanowire on PVDF ultrafiltration membrane performance", *Desalination*, **272**(1-3), 90-97.

Yu, S.C., Chen, Z.W., Cheng, Q.B., Lu, Z.H., Liu, M.H. and Gao, C.J. (2012), "Application of thin-film composite hollow fiber membrane to submerged nanofiltration of anionic dye aqueous solution", *Sep. Purif. Technol.*, **88**, 121-129.

Zhang, M.G., Nguyen, Q.T. and Ping, Z.H. (2009), "Hydrophilic modification of poly (vinylidene fluoride) microporous membrane", *J. Membr. Sci.*, **327**(1-2), 78-86.

Zhang, L.L., He, G.H., Zhao, W., Tan, M. and Li, X.C. (2010a), "Effect of formamide additive on the structure and gas permeation performance of polyethermide membrane", *Sep. Purif. Technol.*, **73**(2), 188-193.

Zhang, H., Zhao, Y.L., Wang, H.T., Zhong, W., Du, Q.G. and Zhu, X.M. (2010b), "Phase behavior of polyetherimide/benzophenone/triethylene glycol ternary system and its application for the preparation of microporous membranes", *J. Membr. Sci.*, **354**(1-2), 101-107.

Zhang, L.L., He, G.H., Zhao, W., Nie, F., Li, X.C. and Tan, M. (2011), "Studies on the coating layer in a PTFPMS/PEI composite membrane for gaseous separation", *J. Membr. Sci.*, **371**(1-2), 141-147.

Zou, T.F., Cai, M., Du, R.H. and Liu, J.K. (2012), "Analyzing the uncertainty of simulation results in accident reconstruction with response surface methodology", *Forensic Sci. Int.*, **216**(1-3), 49-60.

RJ